

RD-R174 397

AN ANALYTICAL MODEL OF AN IMPULSIVE THRUSTER(U) ARNY  
ARMAMENT RESEARCH AND DEVELOPMENT CENTER DOVER NJ  
ARMAMENT ENGINEERING DIRECTORATE E M FRIEDMAN ET AL

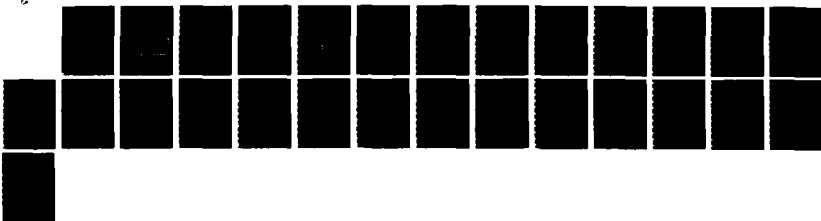
UNCLASSIFIED

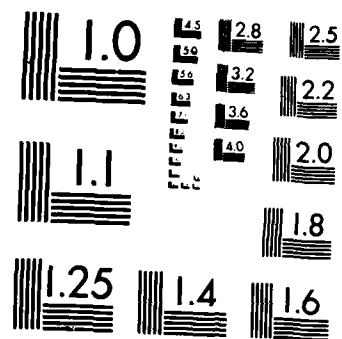
F/G 19/1

1/1

NL

NOV 86 ARAED-TR-86034





MICROCOPY RESOLUTION TEST CHART  
NATIONAL BUREAU OF STANDARDS 1963 A

12

AD-A174 397

AD

AD-E401 601

TECHNICAL REPORT ARAED-TR-86034

AN ANALYTICAL MODEL OF AN IMPULSIVE THRUSTER

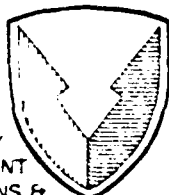
EUGENE M. FRIEDMAN  
MICHAEL J. AMORUSO  
ROMEL CAMPBELL

DTIC  
ELECTED

NOV 25 1986

DTIC FILE COPY

NOVEMBER 1986



US ARMY  
ARMAMENT  
MUNITIONS &  
CHEMICAL COMMAND  
ARMAMENT R&D CENTER

U. S. ARMY ARMAMENT RESEARCH, DEVELOPMENT AND ENGINEERING CENTER  
ARMAMENT ENGINEERING DIRECTORATE  
DOVER, NEW JERSEY

APPROVED FOR PUBLIC RELEASE: DISTRIBUTION IS UNLIMITED.

86 11 25 042

The views, opinions, and/or findings contained in this report are those of the author(s) and should not be construed as an official Department of the Army position, policy, or decision, unless so designated by other documentation.

Destroy this report when no longer needed by any method that will prevent disclosure of contents or reconstruction of the document. Do not return to the originator.

## UNCLASSIFIED

SECURITY CLASSIFICATION OF THIS PAGE (When Data Entered)

REPORT DOCUMENTATION PAGE		READ INSTRUCTIONS BEFORE COMPLETING FORM
1. REPORT NUMBER Technical Report ARAED-TR-86034	2. GOVT ACCESSION NO.	3. RECIPIENT'S CATALOG NUMBER
4. TITLE (and Subtitle)  AN ANALYTICAL MODEL OF AN IMPULSIVE THRUSTER		5. TYPE OF REPORT & PERIOD COVERED  Final
		6. PERFORMING ORG. REPORT NUMBER
7. AUTHOR(s) Eugene M. Friedman Michael J. Amoruso Romel Campbel		8. CONTRACT OR GRANT NUMBER(s)
9. PERFORMING ORGANIZATION NAME AND ADDRESS  ARDEC, AED Armaments Technology Div (SMCAR-AET-A) Dover, NJ 07801		10. PROGRAM ELEMENT, PROJECT, TASK AREA & WORK UNIT NUMBERS
11. CONTROLLING OFFICE NAME AND ADDRESS  ARDEC, IMD STINFO Div (SMCAR-MSI) Dover, NJ 07801		12. REPORT DATE  November 1986
14. MONITORING AGENCY NAME & ADDRESS (if different from Controlling Office)		13. NUMBER OF PAGES  27
		15. SECURITY CLASS. (of this report)  Unclassified
		15a. DECLASSIFICATION/DOWNGRADING SCHEDULE
16. DISTRIBUTION STATEMENT (of this Report)  Approved for public release; distribution unlimited.		
17. DISTRIBUTION STATEMENT (of the abstract entered in Block 20, if different from Report)		
18. SUPPLEMENTARY NOTES		
19. KEY WORDS (Continue on reverse side if necessary and identify by block number)  Flight simulation Analytical simulation Impulsive thruster		
20. ABSTRACT (Continue on reverse side if necessary and identify by block number)  The use of impulsive or nearly impulsive thrusters for the maneuvering force on artillery projectiles has recently been of great interest. The computational cost of numerically integrating the force and torque of distributed thrusters has been high. A method is developed for the one-step application of an exact solution of the flight mechanics for a helical thruster distribution on an axisymmetric body. -4		

ACKNOWLEDGMENT

The authors wish to express their appreciation to Walter Koenig whose efforts contributed immeasurably to the success of this method.

DTIC  
ELECTED  
S NOV 25 1986 D  
B



Accession Form

NTIS	1
DTIC	1
Unclassified	1
Justification	1
Project	1
Directorate	1
Approved	1
Dist	1

A-1

## CONTENTS

	<b>Page</b>
<b>Introduction</b>	1
<b>Analysis</b>	1
<b>Numerical Example</b>	10
<b>Conclusions</b>	10
<b>Symbols</b>	15
<b>Appendix - Program CGSP</b>	17
<b>Distribution List</b>	23

## INTRODUCTION

A great deal of interest has been shown within the Army in recent years in gun fired projectiles which correct their flight paths by impulsive means. One of the more interesting concepts for large caliber projectiles has been an arrangement of propellant-filled helical grooves on the cylindrical portion of the projectile which burn in a progressive manner (from one end to the other). This arrangement has the virtue of controlling the introduction of nutation and precession motion to the flight.

In the flight simulation of such projectiles, the burning of the propellant has historically been modeled as the application of a radial force to the projectile which moves from one end of the groove to the other as the point of burning of the propellant moves. Since the typical speed of burning might be 20,000 feet per second, the integration step size (in time) required to adequately model the shape of the helical groove in space will be quite short compared to the typical rigid body aerodynamic response times of the projectile, causing very large costs in computer time in the flight simulation of the projectile. Therefore, an impulsive analytical model of such a burning process was developed which exactly models the dynamic response of a rigid axisymmetric body to which is applied a radial thrust, moving from one end to the other with a finite burn time. This process is applied as a single step change in the spin components in body fixed coordinates, resulting in large savings in computer time compared to the numerical integration of the rigid body response. This is not an approximation to the rigid body motion under this force alone, but an exact solution; the numerical solution is an approximation to the geometry of the helix. If there is an approximation, it is in the neglect of the aerodynamic forces during the burn time. Aerodynamic forces typically provide approximately two g's of acceleration which is almost entirely axial, while the impulsive thruster typically provides three thousand radial g's during the short duration of the burn. This would appear to amply justify neglect of the lateral aerodynamics during the short application time of the impulse.

## ANALYSIS

The Euler equations of rotational motion of a rigid body can be written as

$$I_x \dot{w}_x - w_y w_z (I_y - I_z) = N_x = 0 \quad (1)$$

$$I_y \dot{w}_y - w_z w_x (I_z - I_x) = N_y = (\bar{x} + \Delta x) F \cos(\theta) \quad (2)$$

$$I_z \dot{w}_z - w_x w_y (I_x - I_y) = N_z = (\bar{x} + \Delta x) F \sin(\theta) \quad (3)$$

where  $N_x = 0$ , since the applied force is radial and exerts no torque about the x-axis, and  $I_y - I_z = 0$  since the body is assumed axially symmetric (fig. 1). The

moment arm due to the instantaneous application of the force of the burning propellant is at  $x + \Delta x$ , where  $\Delta x$  is the displacement between the initiation point of ignition and the center of mass of projectile, and  $x = 0$  at the point of initiation of the burning of the propellant.

Several auxiliary relationships are required for this development (fig. 2). Inspection of this figure reveals that

$$\bar{t} = t - t_0 \quad (4)$$

$$\bar{x} = x - x_M + \Delta x = x - x_0 \quad (5)$$

$$\bar{\theta} = (\theta - \theta_0) = 2 \pi \bar{T}x/D \quad (6)$$

$$\bar{l}^2 = \{ \bar{x}^2 + (r\bar{\theta})^2 \}^{1/2} \quad (7)$$

$$\bar{l} = \bar{x} [1 + (\pi T)^2]^{1/2} \quad (8)$$

where  $\bar{l}$  is the distance down the groove,  $x_0$  is the value of  $x$  at the start of the burn, and  $x$  is zero at the start of the burn. Similarly,  $\bar{t}$  and  $\bar{\theta}$  are both zero at the start of burn. The quantity  $x_M$  is the value for  $x$  at the center of mass and  $\Delta x$  is the displacement in  $x$  between the center of mass and the start of thruster burn. Note from equation 5 that  $x + \Delta x = x - x_M$ .

If the linear burning rate of the propellant is  $R$  feet per second, and it yields  $I$  pound-seconds of thrust per foot of thruster, then

$$F = RI \quad (9)$$

is the force of thrust being applied to the groove at the point of burning at any time during the burning process.

From equation 6

$$dx/dt = -[D/(2\pi T)] d\theta/dt \quad (10)$$

From equation 8

$$d\bar{l}/dt = -d\bar{x}/dt \sqrt{(1 + (\pi T)^2)} \quad (11)$$

but

$$\frac{d\bar{l}}{dt} = R \quad (12)$$

where  $R$  is the linear burning rate.

From equation 1

$$dw_x = 0 \quad (13)$$

for an axially symmetric projectile.

From equation 8

$$\bar{x} = -\bar{l}/ \sqrt{[1 + (\pi T)^2]} = -R\bar{t}/ \sqrt{[1 + (\pi T)^2]} \quad (14)$$

From equations 6 and 14

$$\bar{\theta} = \theta - \theta_0 = +2\pi T \bar{x}/D = -2\pi R \bar{t} / \{ D \sqrt{[1 + (\pi T)^2]} \} \quad (15)$$

Thus, when equations 9, 14, and 15 are applied, equations 2 and 3 become

$$\begin{aligned} I_y \dot{w}_y - w_z w_x (I_z - I_x) &= \{-R\bar{t}/ \sqrt{[1 + (\pi T)^2]} + \Delta x\} * RI * \\ \cos \{-2\pi T R \bar{t} / [D * \sqrt{[1 + (\pi T)^2]}] + \theta_0\} \end{aligned} \quad (16)$$

$$\begin{aligned} I_z \dot{w}_z - w_x w_y (I_x - I_y) &= \{-R\bar{t}/ \sqrt{[1 + (\pi T)^2]} + \Delta x\} * RI * \\ \sin \{-2\pi T R \bar{t} / [D * \sqrt{[1 + (\pi T)^2]}] + \theta_0\} \end{aligned} \quad (17)$$

Define

$$A = -R^2 I / \sqrt{[1 + (\pi T)^2]} \quad (18)$$

$$B = R I \Delta x \quad (19)$$

and

$$K = -2\pi T R / \{ D * \sqrt{[1 + (\pi T)^2]} \} \quad (20)$$

then equations 16 and 17 become

$$I_y \ddot{w}_y - w_z w_x (I_z - I_x) = [\bar{A}t + B] \cos(\bar{K}t + \theta_0) \quad (21)$$

$$I_z \ddot{w}_z - w_y w_x (I_x - I_y) = [\bar{A}t + B] \sin(\bar{K}t + \theta_0) \quad (22)$$

Equations 21 and 22 can be decoupled by differentiating each and substituting the solution for  $\dot{w}_y$  from 22 into the derivative of 21 and the solution for  $\dot{w}_z$  from 21 into the derivative of 22. Keeping in mind that  $w_x = 0$ , the differentiation results in

$$\begin{aligned} I_y \ddot{\dot{w}}_y - \dot{w}_z w_x (I_z - I_x) &= A \cos(\bar{K}t + \theta_0) - AK \bar{t} \sin(\bar{K}t + \theta_0) \\ &- BK \sin(\bar{K}t + \theta_0) \end{aligned} \quad (23)$$

$$\begin{aligned} I_z \ddot{\dot{w}}_z - \dot{w}_y w_x (I_x - I_y) &= A \sin(\bar{K}t + \theta_0) + AK \bar{t} \cos(\bar{K}t + \theta_0) \\ &+ BK \cos(\bar{K}t + \theta_0) \end{aligned} \quad (24)$$

The substitution of the solution of 22 into 23 eliminates  $\dot{w}_z$

$$\begin{aligned} I_y \ddot{\dot{w}}_y + w_x^2 w_y (I_x - I_z) (I_x - I_y) / (I_z) &= \\ \{\bar{A}t[w_x(I_z - I_x) / (I_z) - K] + B[w_x(I_z - I_x) / (I_z) - K]\} \\ \sin(\bar{K}t + \theta_0) + A \cos(\bar{K}t + \theta_0) \end{aligned} \quad (25)$$

while the substitution of the solution of 21 into 24 eliminates  $\dot{w}_y$

$$\begin{aligned} I_z \ddot{\dot{w}}_z + w_x^2 w_z (I_x - I_z) (I_x - I_y) / (I_y) &= \\ \{\bar{A}t[w_x(I_x - I_y) / (I_y) + K] + B[w_x(I_x - I_y) / (I_y) + K]\} \\ \cos(\bar{K}t + \theta_0) + A \sin(\bar{K}t + \theta_0) \end{aligned} \quad (26)$$

For convenience, rewrite 25 as

$$J \ddot{w}_y + M w_y = (\bar{E}t + F) \sin(\bar{K}t + \theta_0) + A \cos(\bar{K}t + \theta_0) \quad (27)$$

where

$$J = I_y \quad (28)$$

$$M = w_x^2(I_x - I_z)(I_x - I_y) / (I_z) \quad (29)$$

$$E = -A[K + w_x(I_x - I_z) / (I_z)] \quad (30)$$

and

$$F = -B[K + w_x(I_x - I_z) / (I_z)] \quad (31)$$

The complete solution to 27 is the sum of the general solution of the equation with the driving terms set to zero and a particular solution of the inhomogeneous equation. The general solution of the homogeneous equation

$$\ddot{J}w_y + Mw_y = 0$$

$$w_y = c_h \cos(\sqrt{\lambda}t + \phi) \quad (32)$$

which, if substituted back into the homogeneous equation, yields the secular equation

$$-\lambda^2 J + M = 0 \quad (33)$$

or

$$\lambda = \sqrt{(M/J)} \quad (34)$$

A particular solution of the inhomogeneous equation is needed. Try an expression of the form

$$w_y = c_1 \sin(Kt + \theta_0) + c_2 \cos(Kt + \theta_0) + c_3 t \sin(Kt + \theta_0) + c_4 t \cos(Kt + \theta_0) \quad (35)$$

Differentiate 35 twice to obtain  $\ddot{w}_y$ , then substitute it and 35 into 27 to evaluate  $c_1$ ,  $c_2$ ,  $c_3$ , and  $c_4$ . We get

$$-c_1 K^2 J - 2c_4 KJ + Mc_1 = F \quad (36)$$

$$-c_3 K^2 J + M c_3 = E \quad (37)$$

$$-c_2 K^2 J + 2c_3 KJ + c_2 M = A \quad (38)$$

$$-c_4 K^2 J + M c_4 = 0 \quad (39)$$

From 39, if  $J K^2 - M \neq 0$ , (i.e.,  $K \neq \lambda$ , cf. equation 33)

$$c_4 = 0 \quad (40)$$

From 40 and 36,

$$M c_1 - JK^2 c_1 = F$$

or using 34 to eliminate M

$$c_1 = F / (M - JK^2) = F / [J(\lambda^2 - K^2)] \quad (41)$$

From 37

$$c_3 = E / (M - K^2 J) = E / [J(\lambda^2 - K^2)] \quad (42)$$

From 38 and 42

$$c_2 = [A(\lambda^2 - K^2) - 2KE] / [J(\lambda^2 - K^2)^2] \quad (43)$$

Therefore 35 simplifies to

$$w_y = c_1 \sin(Kt + \theta_0) + c_2 \cos(Kt + \theta_0) + c_3 t \sin(Kt + \theta_0) \quad (44)$$

and the complete solution is the sum of 44 and 32

$$\begin{aligned} w_y &= c_h \cos(\lambda t + \phi) + c_1 \sin(Kt + \theta_0) + c_2 \cos(Kt + \theta_0) \\ &\quad + c_3 t \sin(Kt + \theta_0) \end{aligned}$$

which can be rewritten as

$$\begin{aligned} w_y &= c_5 \cos(\bar{t}) + c_6 \sin(\bar{t}) + c_1 \sin(K\bar{t} + \theta_0) + c_2 \cos(K\bar{t} + \theta_0) \\ &+ c_3 \bar{t} \sin(K\bar{t} + \theta_0) \end{aligned} \quad (45)$$

The constants of integration  $c_5$  and  $c_6$  can be evaluated in terms of the initial conditions  $w_{y0}$  and  $\dot{w}_{y0}$ . Recall that  $c_1$ ,  $c_2$ , and  $c_3$  are already determined; see 41, 42, and 43.

$$w_{y0} = w_{y0}[t = t_c - L/(2R)] = w_{y0}[\bar{t} = 0] \quad (46)$$

$$\dot{w}_{y0} = \dot{w}_{y0}[t = t_c - L/(2R)] = \dot{w}_{y0}[\bar{t} = 0] \quad (47)$$

where  $t_c$  is the center time, the time of the middle of the burn. For convenience, make the definition

$$\tau = L/R \quad (48)$$

which is the burn time of a thruster. Thus the initial conditions become

$$w_{y0} = w_{y0}(t = t_c - \tau/2) = w_{y0}(\bar{t} = 0) \quad (49)$$

$$\dot{w}_{y0} = \dot{w}_{y0}(t = t_c - \tau/2) = \dot{w}_{y0}(\bar{t} = 0) \quad (50)$$

The derivative of 45 is

$$\begin{aligned} \dot{w}_y(\bar{t}) &= -\lambda c_5 \sin(\lambda \bar{t}) + \lambda c_6 \cos(\lambda \bar{t}) + K c_1 \cos(K\bar{t} + \theta_0) \\ &- K c_2 \sin(K\bar{t} + \theta_0) + c_3 \sin(K\bar{t} + \theta_0) + c_3 K \bar{t} \cos(K\bar{t} + \theta_0) \end{aligned} \quad (51)$$

Thus, at  $t = t_c - \tau/2$ , or  $\bar{t} = 0$

$$w_{y0} = c_5 + c_1 \sin[\theta_0] + c_2 \cos[\theta_0] \quad (52)$$

and

$$\dot{w}_{y0} = \lambda c_6 + K c_1 \cos[\theta_0] - K c_2 \sin[\sin \theta_0] + c_3 \sin[\theta_0] \quad (53)$$

Solving for  $c_6$  from 53

$$c_6 = [1/\lambda] \{ \dot{w}_{y0} - Kc_1 \cos[\theta_0] + Kc_2 \sin[\theta_0] - c_3 \sin[\theta_0] \} \quad (54)$$

Solving 52 for  $c_5$

$$c_5 = \{ w_{y0} - c_1 \sin[\theta_0] - c_2 \cos[\theta_0] \} \quad (55)$$

Similarly, the solution to 26 is required

$$\ddot{J}w_z + \bar{M}w_z = (\bar{E}t + \bar{F}) \cos(Kt + \theta_0) + A \sin(Kt + \theta_0) \quad (56)$$

where

$$\bar{J} = I_z = J (I_z/I_y) \quad (57)$$

$$\bar{M} = w_x^2 (I_x - I_z) (I_x - I_y) / I_y = M (I_z/I_y) \quad (58)$$

$$\bar{E} = A [K + w_x (I_x - I_y) / I_y] \quad (59)$$

$$\bar{F} = B [K + w_x (I_x - I_y) / I_y] \quad (60)$$

The homogeneous part of 56 is formally identical to the homogeneous part of 27; therefore the homogeneous solution of 56 is formally the same as the homogeneous solution of 27 which is expressed by 32 and 34. For the inhomogeneous solution, again try the form of 35

$$w_z = \bar{c}_1 \sin(Kt + \theta_0) + \bar{c}_2 \cos(Kt + \theta_0) + \bar{c}_3 t \sin(Kt + \theta_0) + \bar{c}_4 t \cos(Kt + \theta_0) \quad (61)$$

Similarly, differentiate twice and substitute into the differential equation, in this case 56, yielding

$$\bar{c}_1 = [A(\bar{M} - K\bar{J}) + 2\bar{J}\bar{K}\bar{E}] / [\bar{M} - K^2\bar{J}]^2$$

or since  $M/J = M/J = \lambda^2$ , then

$$\bar{c}_1 = [A(\lambda^2 - K^2) + 2KE] / [\bar{J}(\lambda^2 - K^2)^2] \quad (62)$$

$$\bar{c}_2 = \bar{F}/[\bar{M} - K^2\bar{J}] = \bar{F}/[\bar{J}(\lambda^2 - K^2)] \quad (63)$$

$$\bar{c}_3 = 0 \quad (64)$$

and

$$\bar{c}_4 = E/(\bar{M} - K^2\bar{J}) = \bar{E}/[\bar{J}(\lambda^2 - K^2)] \quad (65)$$

which should be compared to 40 through 43. Following the pattern used to evaluate the constants of integration in equation 45, first write the recase complete solution of 56, which is analogous to 45, as

$$w_z = \bar{c}_5 \cos(\lambda \bar{t}) + \bar{c}_6 \sin(\lambda \bar{t}) + \bar{c}_1 \sin(K \bar{t} + \theta_0) + \bar{c}_2 \cos(K \bar{t} + \theta_0) \\ + \bar{c}_4 \bar{t} \cos(K \bar{t} + \theta_0) \quad (66)$$

where

$$\bar{c}_5 = \{w_{z0} - \bar{c}_1 \sin[\theta_0] - \bar{c}_2 \cos[\theta_0]\} \quad (67)$$

and

$$\bar{c}_6 = [1/\lambda] \{\dot{w}_{z0} - K\bar{c}_1 \cos[\theta_0] + K\bar{c}_2 \sin[\theta_0] - \bar{c}_4 \cos[\theta_0]\} \quad (68)$$

To obtain the final result, evaluate 45 and 66 at  $t = t_c - \tau/2$  or, equivalently, at  $\bar{t} = \tau = L/R$ .

$$w_y = c_5 \cos[\lambda L/R] + c_6 \sin[\lambda L/R] + c_1 \sin[KL/R + \theta_0] \\ + c_2 \cos[KL/R + \theta_0] + c_3 [L/R] \sin[KL/R + \theta_0] \quad (69)$$

$$w_z = \bar{c}_5 \cos[\lambda L/R] + \bar{c}_6 \sin[\lambda L/R] + \bar{c}_1 \sin[KL/R + \theta_0] \\ + \bar{c}_2 \cos[KL/R + \theta_0] + \bar{c}_4 [L/R] \cos[KL/R + \theta_0] \quad (70)$$

Care must be taken in specifying initial conditions. The original equations to be solved were the coupled first order equations 2 and 3. For these equations, only  $w_{yo}$  and  $w_{zo}$  need to be specified. However, when the equations are decoupled, the order is increased and the initial conditions,  $w_y$  and  $w_z$ , are also required. These cannot be specified arbitrarily. Instead, to avoid spurious solutions and to assure consistency with the original coupled first order equations 2 and 3,  $w_y$  and  $w_z$  in principle must be calculated from  $w_{yo}$  and  $w_{zo}$  using equations 2 and 3. Equivalently, equations 21 and 22 can be solved for  $w_y$  and  $w_z$  with  $t$  set to zero to yield the required initial conditions, viz.

$$\dot{w}_{yo} = \{w_{zo} w_x [I_z - I_x] + B \cos \theta_o\} / I_y \quad (71)$$

$$\dot{w}_{zo} = \{w_{yo} w_x [I_x - I_y] + B \sin \theta_o\} / I_z \quad (72)$$

where  $B$  could be replaced by  $R I \Delta x$ . (See equation 19.) A program implementing this approach is in the appendix.

#### NUMERICAL EXAMPLE

The analytical approach described above was tested by comparison to numerical integration of equations 2 and 3 using a fourth order Runge-Kutta integration technique. These results are reported in table 1. The first entry is the exact result obtained by the analytical technique. The second entry represents numerical integration using an integration time step of 0.00000001 second. Results are interpolated to yield a value at the exact time of the end of burn. (If the simulations are adjusted to make them stop at the same time, the numerical and analytical results for  $w_y$  and  $w_z$  agree to at least eight significant figures.) The third and fourth table entries use integration time steps of 0.0000001 second and 0.000001 second, respectively. Note that the results obtained numerically required from 23 to 2085 times the computer CPU time as the new analytical approach to obtain 3 to 6 significant figure accuracy, respectively.

#### CONCLUSIONS

The closed form, analytical solution has been accurate and highly efficient for the simulation of the flight of projectiles with maneuvers implemented by helical, quasi-impulsive thrusters. The technique will be implemented in the further development of such projectiles at ARDEC.

Table 1. Comparison of results

<u>Model type</u>	<u>Time step (sec)</u>	<u>CPU time (sec)</u>	<u>w<sub>y</sub> (rad)</u>	<u>w<sub>z</sub> (rad)</u>
Analytical	N/A	0.0106	0.53275603	-0.41630908
Numerical	$10^{-8}$	22.096	0.53275601	-0.41630910
Numerical	$10^{-7}$	2.278	0.53275061	-0.41631581
Numerical	$10^{-6}$	0.246	0.53234719	-0.41681537

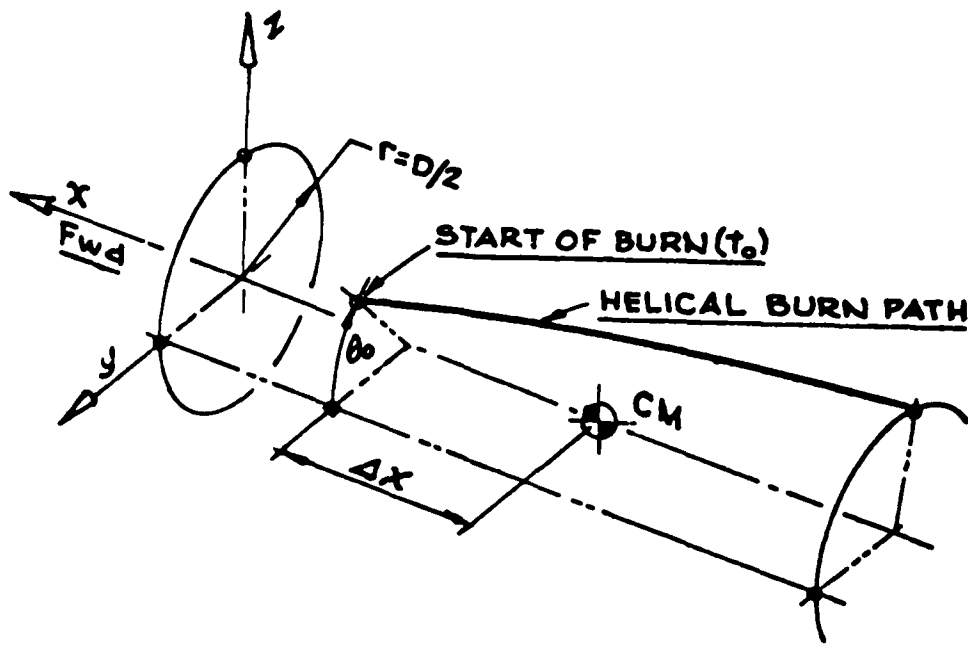
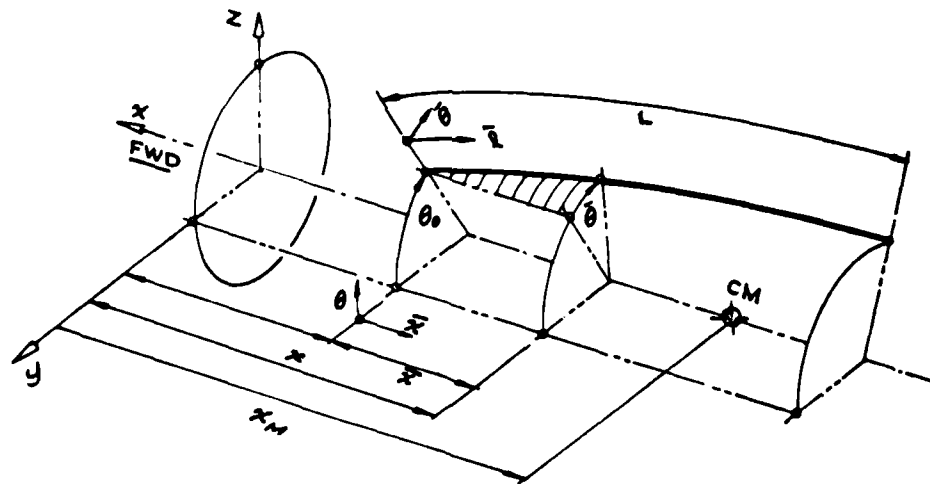


Figure 1. Helical burn path for projectile thruster



$$\begin{array}{ll}
 \bar{t}=0 & x=0 \\
 t=t_0 & x=x_0 \\
 \bar{t}=t-t_0 & x=x-x_m - \Delta x \\
 & x=x-x_0 \\
 & x=x-x_0 - x_0 \\
 & x=x-x_0 - x_0 - \Delta x
 \end{array}
 \quad
 \begin{array}{ll}
 \theta=0 \\
 \theta=\theta_0 \\
 \theta=\theta-\theta_0 \\
 \theta=\frac{2\pi T}{D}x \\
 \theta=0
 \end{array}
 \quad
 \begin{array}{l}
 L=-x\sqrt{1+(\pi T)^2} \\
 L^2=x^2+(r\theta)^2
 \end{array}$$

Figure 2. Coordinate system relationships

## SYMBOLS

F	Force applied to body by burning propellant (pounds)
D	Diameter of cylindrical body section (feet)
I	Specific impulse of thruster (pound-seconds/foot of thruster)
$I_x, I_y, I_z$	Moments of inertia about fixed axes of body (slug-feet squared)
l	Distance down groove (feet)
L	Total length of thruster groove (feet)
$N_x, N_y, N_z$	Components of torque applied to body (pound-feet)
R	Linear burning rate of propellant (feet/second)
t	Time (seconds)
$\bar{t}$	Time measured from zero at start of burn (seconds)
$t_c$	Time $t$ at center of thruster burn
T	Twist of helix (turns per caliber)
$\bar{x}, \bar{y}$	Coordinates of point on groove when "unwrapped" (feet)
x, y, z	Coordinates of point in body frame (feet)
$\theta$	Polar angle of point on groove, positive from Y toward Z (radians)
$\tau$	Time of a thruster burn (seconds)
$\lambda$	Natural frequency of solution to homogeneous differential equation (per second)
$w_x, w_y, w_z$	Components of spin in body frame (radians per second)

**APPENDIX**  
**PROGRAM CGSP**

```

C
C THIS IS A SAMPLE DRIVER PROGRAM FOR TESTING SUBROUTINE OMEGA
C
C COMMON R,L,I,T,D,WX,IX,IY,IZ,PI,WYZERO,WZZERO,WYZDOT,WZZDOT,
+ THZER,XZERO,FREQN,FREQF
  REAL L,I,IX,IY,IZ
C
C DEFINITIONS
C
  R=2.2310E04
  L=1.333
  I=12.842
  T=-1.5755E-02
  D=.4199
  WX=1000.0
  IX=.136
  IY=.930
  IZ=IY
  PI=3.141592654
C
C BURN OUT TIME. THE FOLLOWING EXACT VALUE MAY BE REPLACED
C BY THE ACTUAL INTEGRATION CUT OFF TIME IN A NUMERICAL
C INTEGRATION ROUTINE FOR PURPOSES OF COMPARISON.
C
  TIME = L/R
C
C INITIAL CONDITIONS
C
  WYZERO = 0.1
  WZZERO = 0.2
C
  XZERO = 0.66667
  THZER = PI/7.
C
  CALL OMEGA(TIME,WY,WZ)
  PRINT*, '          TIME           WY           WZ'
  WRITE(*,100) TIME,WY,WZ
  WRITE(*,101)
1 CONTINUE
  STOP
100 FORMAT(4F15.12,//)
101 FORMAT('1')
END
  SUBROUTINE OMEGA(TIME,WY,WZ)
  COMMON R,L,I,T,D,WX,IX,IY,IZ,PI,WYZERO,WZZERO,WYZDOT,WZZDOT
+ ,THZER,XZERO,FREQN,FREQF
  REAL L,I,IX,IY,IZ,J,JBAR
C
C FREQN = NATURAL FREQUENCY OF THE SYSTEM
C FREQF = FORCING FUNCTION FREQUENCY

```

```

C
EL=SQRT(1. + (PI*T)*(PI*T))
FREQN=SQRT((WX*WX)*(IX-IZ)*(IX-IY)/(IY*IZ) )
FREQF = -(2. * PI * T * R )/( D*EL )
J=IY
JBAR=IZ
A=-(R*R) * I/EL
B= R * I * XZERO
E= -A * ((WX * (IX-IZ)/IZ) + FREQF)
EBAR= +A * ((WX * (IX-IY)/IY) + FREQF)
F= -B * ((WX * (IX-IZ)/IZ) + FREQF)
FBAR= B * ((WX * (IX-IY)/IY) + FREQF)
DENOM= (FREQN*FREQN) - (FREQF*FREQF)

C
C CONSTANTS DERIVED FROM THE DECOUPLING PROCESS.
C
C1=F/(J*DENOM)
C2B=FBAR/(JBAR*DENOM)
C2=(A/(J*DENOM))-(E*2.*FREQF/(J*(DENOM*DENOM)))
C1B=(A/(JBAR*DENOM))+(EBAR*2.*FREQF/(JBAR*(DENOM*DENOM)))
C3=E/(J*DENOM)
C4B=EBAR/(JBAR*DENOM)
C4=0.
C3B=0.

C
C SUPPRESS SPURIOUS SOLUTIONS INTRODUCED BY
C TAKING SECOND DERIVATIVES OF WY AND WZ
C
WYZDOT = (WZZERO*WX*(IZ-IX) + B*COS(THZER))/IY
WZZDOT = (WYZERO*WX*(IX-IY) + B*SIN(THZER))/IZ

C
C CONSTANTS DERIVED FROM THE INITIAL CONDITIONS
C
C5= (WYZERO-C1*SIN(THZER)-C2*COS(THZER) )
C6 = (1./FREQN)*(WYZDOT-FREQF*C1*COS(THZER)
+ +FREQF*C2*SIN(THZER) - C3*SIN(THZER) )
C5B= (WZZERO-C1B*SIN(THZER) -C2B*COS(THZER) )
C6B = (1./FREQN)*(WZZDOT
+ -FREQF*C1B*COS(THZER)+FREQF*C2B*SIN(THZER)-C4B*COS(THZER) )

C
WY = C5*COS(FREQN*TIME) + C6*SIN(FREQN*TIME)
+ + C1*SIN(FREQF*TIME+THZER) +
+ C2*COS(FREQF*TIME+THZER) + C3*TIME*SIN(FREQF*TIME+THZER)

C
WZ = C5B*COS(FREQN*TIME) + C6B*SIN(FREQN*TIME)
+ + C1B*SIN(FREQF*TIME+THZER) + C2B*COS(FREQF*TIME+THZER)
+ +C4B*TIME*COS(FREQF*TIME+THZER)

C
RETURN
END

```

Sample Execution

TIME	WY	WZ
0.00009748991	0.532756032730	-0.416309075410

DISTRIBUTION LIST

Commander  
Armament Research, Development and  
Engineering Center  
U.S. Army Armament, Munitions  
and Chemical Command  
ATTN: SMCAR-MSI (5)  
    SMCAR-AE, B. Bushey  
    SMCAR-AET, W. Ebihara  
    SMCAR-AET-A, A. Loeb (4)  
        D. Mertz (10)  
        R. Kline (3)  
        E. Friedman (3)  
        M. Amoruso (3)  
        R. Campbell (3)  
        W. Koenig  
        C. Ng  
        H. Hudgins  
        E. Brown  
        L. Yee  
    SMCAR-CC, Commander/Director  
        S. Hirshman  
    SMCAR-CCL, J. Gehbauer  
        M. Barbarisi  
    SMCAR-FS, Commander/Director  
        T. Davidson  
    SMCAR-FSA-IM, S. Harnett  
        F. Brody  
        R. Hill  
    SMCAR-FSA-M, R. Botticelli  
    SMCAR-FSF, J. Lehman  
    SMCAR-FSN-N, C. Spinelli  
        J. Sacco  
    SMCAR-FSS, J. Gregoritis  
    SMCAR-FSP, F. Scerbo (4)  
        E. Zimpo  
        D. Ladd

Dover, NJ 07801-5001

Commander  
U.S. Army Armament, Munitions  
and Chemical Command  
ATTN: AMSMC-GCL(D)  
Dover, NJ 07801-5001

Administrator  
Defense Technical Information Center  
ATTN: Accessions Division (12)  
Cameron Station  
Alexandria, VA 22304-6145

**Director**  
U.S. Army Materiel Systems  
Analysis Activity  
ATTN: AMXSY-MP  
Aberdeen Proving Ground, MD 21005-5066

**Commander**  
Chemical Research and Development Center  
U.S. Army Armament, Munitions  
and Chemical Command  
ATTN: SMCCR-SPS-IL  
Aberdeen Proving Ground, MD 21010-5423

**Commander**  
Chemical Research and Development Center  
U.S. Army Armament Munitions  
and Chemical Command  
ATTN: SMCCR-RSP-A  
Aberdeen Proving Ground, MD 21010-5423

**Director**  
Ballistic Research Laboratory  
ATTN: AMXBR-OD-ST  
    AMXBR-BLL, C. Murphy  
    W. Mermagen  
    R. Lieske  
    V. Oskay  
    W. Sturek  
Aberdeen Proving Ground, MD 21005-5066

**Chief**  
Benet Weapons Laboratory, CCAC  
Armament Research and Development Center  
U.S. Army Armament, Munitions  
and Chemical Command  
ATTN: SMCAR-CCB-TL  
Watervliet, NY 12189-5000

**Commander**  
U.S. Army Armament, Munitions  
and Chemical Command  
ATTN: SMCAR-ESP-L  
    AMSMC-PDM  
    AMSMC-ASI  
Rock Island, IL 61299-6000

**Director**  
U.S. Army TRADOC Systems  
Analysis Activity  
ATTN: ATAA-SL  
White Sands Missile Range, NM 88002

Department of the Army  
ATTN: DAMA-CSM  
DAMO-RQS  
Washington, DC 23014

Commander  
U.S. Army Material Command  
ATTN: AMCDE-DM  
5001 Eisenhower Avenue  
Alexandria, VA 22304

Project Manager  
Cannon Artillery Weapons Systems  
ATTN: AMCPM-CAWS  
Dover, NJ 07801-5001

Commander  
Harry Diamond Laboratories  
ATTN: DELHD-DCB, J. Miller  
M. Probst  
Adelphi, MD 20783-1197

Headquarters  
Air Force Weapons Laboratory (WLX)  
ATTN: Technical Library  
Kirtland Air Force Base, NM 87117

Headquarters  
U.S. Army Training and Doctrine Command  
ATTN: ATCD-MC  
ATAA-SL  
Ft. Monroe, VA 23651

Director  
Marine Corps Development and Engineering  
Command  
ATTN: Code D092  
Quantico, VA 22134

Headquarters  
Eglin Air Force Base  
ATTN: Technical Library  
Eglin Air Force Base, FL 32542

Commander  
U.S. Army Test and Evaluation Command  
ATTN: DRSTE-CT-T  
Aberdeen Proving Ground, MD 21005

Commander  
U.S. Naval Weapons Center  
ATTN: Technical Library (Code 5557)  
China Lake, CA 93555

Commander  
U.S. Naval Surface Weapons Center  
White Oak Laboratory  
ATTN: Research Library  
Silver Spring, MD 20910

Commander  
U.S. Naval Surface Weapons Center  
Dahlgren Laboratory  
ATTN: Technical Library  
Dahlgren, VA 22448

Commander/Director  
U.S. Naval Ship Research and Development  
Center  
ATTN: Technical Library  
Washington, DC 20007

Commanding General  
U.S. Army Missile Command  
ATTN: Technical Library, R. Deep  
Redstone Arsenal, AL 35809

Sandia National Laboratories  
Division 1631  
ATTN: A. Hodapp  
R. LaFarge  
P.O. Box 5800  
Albuquerque, NM 87185

Sandia National Laboratories  
Division 8152  
ATTN: D. Beyer  
P.O. Box 969  
Livermore, CA 94550

Raytheon Company  
Missile Systems Division  
ATTN: Vincent A. Grosso  
Marilyn Kloss  
Hartwell Rd  
Bedford, MA

E N D

/ — 81

D T I C